Vietnam Journal of Science and Technology ***55*** *(6A) (2017) 72-82*

ABSORPTION OF SOME SMALL SILVER CLUSTERS: DFT AND CASPT2 CALCULATIONS

Ngo Tuan Cuong[1, *] Nguyen Thanh Tung[2], Nguyen Minh Tam[3]

[1]*Center for Computational Science, Hanoi National University of Education, 136 Xuan Thuy, Cau Giay, Ha Noi*
[2]*Institute of Material Science, VAST, 18 Hoang Quoc Viet, Cau Giay, Ha Noi*
[3]*Computational Chemistry Research Group, Ton Duc Thang University, 19 Nguyen Huu Tho, Tan Hung, District 7, Ho Chi Minh City*

[*]Email: *cuongnt@hnue.edu.vn*

Received : 15 June 2017; Accepted for publication : 21 December 2017

ABSTRACT

Two quantum chemical methods which are the time-dependent density functional theory (TD-DFT) and the complete active space CASPT2/CASSCF have been used in modeling absorption spectra of silver clusters Ag_n (n = 2, 3, 4, 6, 8). There is an overall good agreement between TD-DFT and CASPT2 results for transition energies. The absorption spectra of the Ag_n clusters examined can reasonably be simulated using the excitation energies obtained by either TD-DFT or CASPT2 method. The main result emerged from this calculation is that the TD-DFT method is suitable for treatment of excited states of Ag clusters. The choice of specific functionals and basis sets to be used in some cases induces important effects on the calculated spectra. It is also noteworthy to mention that for some clusters, the neutral Ag_6 for instance, the effect of noble gas environment is significant, while for some others such as the neutral Ag_8, it is not. Therefore, carrying out TD-DFT calculations to reproduce and to assign a given structure to an experimental absorption spectrum of a silver cluster, it is not only to select suitable functionals but also to take enough effects of environments into account.

Keywords: silver clusters, absorptionspectra, TD-DFT computations, CASSCF/CASCASPT2.

1. INTRODUCTION

Clusters of silver atom and ions have recently attracted the interest of scientists because of their pronounced catalytic and emissive properties. While the silver single atom can only exist in two oxidation states, either 0 or +1, those clusters can be formed in different oxidation states. As a result, this influences to their optical properties. Due to the strong luminescence in the UV-VIS region, silver clusters display a potential for applications in material sciences and biomedicine [1-4].

The structures, optical absorption and fluorescence spectra in the UV-visible range of selected neutral Ag_n clusters (n = 1-9) in solid neon were recently recorded and compared to

those of theoretical spectra as well [5-18]. Although that studies confirmed the power of computation in the exploring properties of silver clusters, it is requested more computational investigations to clearly understand the properties of silver clusters in order to support experiments in new silver cluster based compounds/devices. In this context, we set out to determine, as for a preliminary calibration, the electronic structures and absorption spectra of some small pure silver clusters Ag_n, using both TD-DFT and CASSCF/CASPT2 methods.

2. MATERIALS AND METHODS

2.1. The method of Time-Dependent Density Functional Theory (TDDFT)

The TD-DFT method [19-23] is a widely used method for treating excited states. In this work, we simulate the absorption spectra using the TD-DFT method implemented in the Gaussian 09 package [24] using the following procedure: i) First, a density functional theory (DFT) calculation is used for geometry optimization, followed by harmonic vibrational frequency calculation; ii) Second, the TD-DFT calculation is performed at the optimized geometry to determine the energy levels of the excited states and absorption spectra of the clusters.

2.2. The multiconfigurational method

The procedure to model the absorption using the CASPT2/CASSCF and RASSI methods, implemented in the MOLCAS package [25] is described as following: First, a fixed molecular geometry obtained by the DFT optimization is chosen. Second, the GATEWAY module is performed to collect the information about the molecular system such as the symmetry, basis set, for all the subsequent calculations. Third, the SEWARD module is performed to generate and to store the one- and two-electron integrals which are always required in the subsequent SCF calculation. Fourth, the SCF module is performed to obtain the Hartree-Fock SCF wave function and energy. Fifth, the CASSCF computation is carried out to generate the multiconfigurational wave functions. Sixth, the CASPT2 calculation follows the CASSCF one to give a second-order perturbation estimate of the full CI energy using the CASSCF wave function as the reference. Lastly, the RASSI method is used to compute matrix elements of electronic transition dipole moments, and thereby oscillator strengths (*f*).

3. RESULTS AND DISCUSSION

3.1. Ag_2 Neutral Dimer

Let us start our modeling with the neutral dimer Ag_2. We have employed six functionals including the hybrid B3LYP and CAM-B3LYP, the pure BP86, PBE1PBE and LC-wPBE and the meta-GGA M06 [26-31], in conjunction with the correlation consistent aug-cc-pVDZ-PP basis set for silver [32]. Each functional is used to optimize geometries, calculate the vertical ionization energies and vertical electron affinities, and the absorption spectra. The obtained results are then compared with the available experimental and previous calculated results.

The results of our calculations listed in Table 1 show that the B3LYP, CAM-B3LYP and M06 functionals give good IEv and VDE values, while the BP86, PBE1PBE and LC-wPBE do not. The TD-DFT method using the above functionals has been used to calculate the absorption

spectrum of the neutral silver dimer. The results are summarized in Table 2 and illustrated in Figure 1. Table 2 shows that for Ag_2, calculations using the B3LYP functional reproduce quite well the experimental results for the $^1\Sigma_g^+ \rightarrow {}^1\Sigma_u^+$ and $^1\Sigma_g^+ \rightarrow {}^1\Pi_u$ electronic transitions. The TD-B3LYP/aug-cc-pVDZ-PP calculation results are also agree well with the results obtained from previous calculations using the method of equation-of-motion coupled-cluster theory including single and double excitations (EOM-CCSD) [15].

We have also performed the single point CASPT2/CASSCF calculations for the absorption spectrum of Ag_2. Two basis sets have been used in this calculation, namely, the ANO-RCC-Large [33] basis set, and the effective core potential (ECP) basis set of Dolg et al. [34]. The active spaces consist of distributions of two electrons amongst eight (CASSCF(2,8)) and fourteen (CASSCF(2,14)) orbitals including 5*s* and 5*p* atomic orbitals of silver atoms. Results of the CASPT2/CASSCF calculations are listed in Table 2.

It turns out that the location of the S_1 state is similarly reproduced by all six DFT functionals at around 3.0 eV. The CASPT2 results appear to be less dependent on the active space. On the contrary, the difference between the transition energies obtained by the two basis sets is larger (Table 2).

For the sake of simplicity, only the TDB3LYP/aug-cc-pVDZ-PP result is displayed in Figure 1. At this level, the absorption spectrum of silver dimer contains two distinct bands which center at 410 nm (~3.0 eV) and 272 nm (~4.6 eV) wavelengths. The longer wavelength absorption band is due to the HOMO → LUMO transition ($S_0 \rightarrow S_1$). Experimentally, an absorption band at 2.85 eV has been assigned for Ag_2 [8-9]. Table 2 points out that either the TD-DFT values of ~3.0 eV or the CASPT2/ECP values of ~2.9 eV reproduce quite well the experimental result. Our calculated results are also comparable to the previous EOM-CCSD value of 2.94 eV [15]. The shorter wavelength absorption band (Figure 1) is due to the $S_0 \rightarrow S_2$ transition. Experimentally, the values of 4.67 and 4.84 eV [12-13] have been assigned for the associated absorption band. In this case, both TD-DFT and CASPT2/ECP results (4.2 – 4.6 eV) appear to be underestimated, whereas the CASPT2/ANO-RCC appear to reproduce better (4.7 - 4.8 eV) this energetic parameter.

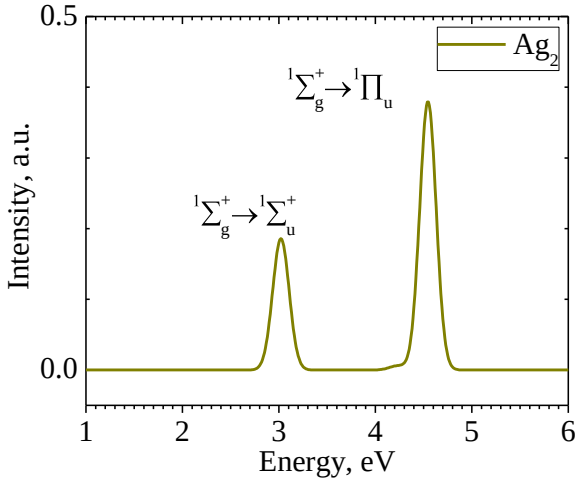

Figure 1. Absorption spectrum of neutral silver dimer Ag_2 simulated by the TD-B3LYP/aug-cc-pVDZ-PP calculation.

Table 1. Bond distance (angström), vertical electron detachment (VDE), vertical electron affinity (EAv) and vertical ionization energy (IEv) of silver dimer Ag_2 and trimer Ag_3, calculated by DFT using different functional and compared with experiment. Values are given in eV.

Method (functional)	Silver dimer Ag_2			Silver trimer Ag_3		
	d(Ag-Ag), Å	VDE	IE_v	d(Ag-Ag), Å	EA_v (VDE)	IE_v
B3LYP	2.585	1.17	7.92	2.714	2.39	7.01
CAM-B3LYP	2.560	1.08	7.72	2.688	2.27	6.54
BP86	2.553	1.32	8.24	2.668	2.57	7.16
M06	2.585	1.14	7.90	2.714	2.46	6.86
PBE1PBE	2.565	1.01	7.67	2.686	2.11	5.78
LC-wPBE	2.547	0.90	7.21	2.671	1.74	5.42
Experiment		1.10[a]	7.66[b,(*)]		2.43[a]	6.2[c (*)]

[a] Ref. [8]; [b] Ref. [9]; [c]. Ref. [10]; (*) The experimental ionization energy is the adiabatic value, IE_a.

Table 2. Energies of the vertical electronic transition from the ground state (GS) to the singlet excited states (S_1, S_2), as well as triplet excited states (T_1, T_2) of Ag_2. Results are obtained from TD-DFT calculations using the six different functionals in conjunction with the aug-cc-pVDZ-PP basis set, and from CASPT2/CASSCF calculations. Comparison is made with available experimental and previous calculated results.

Method/Functional	T_1, eV	S_1 ($^1\Sigma_g^+ \rightarrow {}^1\Sigma_u^+$), eV	T_2, eV	S_2 ($^1\Sigma_g^+ \rightarrow {}^1\Pi_u$), eV
B3LYP	1.70	3.04	3.66	4.56
CAM-B3LYP	1.55	3.01	3.46	4.34
BP86	1.73	3.02	3.33	4.68
M06	1.76	3.01	3.78	4.40
PBE1PBE	1.62	3.06	3.43	4.40
LC-wPBE	1.46	3.06	2.95	4.24
CASPT2/CASSCF(2/8)/ANO-RCC Large	1.87	3.17	3.79	4.79
CASPT2/CASSCF(2/14)/ANO-RCC Large	1.77	3.14	3.68	4.73
CASPT2/CASSCF(2/8)/ECP-Dolg	1.83	2.93	3.18	4.30
CASPT2/CASSCF(2/14)/ECP-Dolg	1.67	2.87	3.06	4.23
Experiment		2.85[a,b]; 2.94[e]		4.67[b,c,d]; 4.84[b,d]; 4.49[e]

[a] Ref.[11] ; [b] Ref.[12], [c] Ref.[13], [d] Ref.[14], e) Values obtained by the EOM-CCSD calculation, Ref.[15].

3.2. Ag_3 Trimer

We have calculated the vertical electron affinity (EA_v) and the vertical ionization energy (IE_v) of the neutral silver trimer Ag_3 by DFT method using the six different functionals mentioned in Section 3.1. The energetic results are also summarized in Table 1 in comparison with experiment and previous calculations. The TD-DFT calculations as well as CASPT2 calculations have been performed on the silver trimer cation Ag_3^+ in order to probe its absorption

spectrum, which was recorded experimentally [11]. The results are represented in Table 3. The absorption spectrum of Ag_3^+ is characterized by an intense band centered at ~4.0 eV, according to TDDFT calculations using all six functionals. Table 3 points out that the B3LYP functional underestimates the transition energy of the $S_0 \rightarrow S_1$ electronic transition by about 0.4 eV, whereas the LC-wPBE functional gives better result, being 4.1 eV as compared to the experimental one of 4.2 eV, and to the earlier EOM-CCSD result of 4.1 eV [11,15]. The absorption band is due to a dominant contribution from HOMO → LUMO excitation, and a considerably smaller contribution from HOMO-1 → LUMO. For the CASPT2/CASSCF calculation, the active space is the distribution of two electrons amongst twelve MOs and is denoted as CASSCF(2/12). Our CASPT2/CASSCF(2/12) calculations using the two basis sets also provide the transition energy of ~4.0 eV for the $S_0 \rightarrow S_1$ electronic transition of Ag_3^+ which is in good agreement with either experiment or the EOM-CCSD result [11,15] (cf. Table 3).

Table 3. Energies (eV) of the vertical electronic transition from the ground state (GS) to the first (S_1) and second (S_2) singlet excited states, and to the first triplet (T_1) excited state of the cation silver trimer Ag_3^+. Results are obtained from the TD-DFT and from CASPT2/CASSCF(2/12) calculations.

Method/functional	T_1 (^{3}E')	S_1 (^{1}E') (*f*)	S_2 (^{1}E') (*f*)
B3LYP	2.74	3.79 (0.25)	4.62 (0.015)
CAM-B3LYP	2.77	3.92 (0.27)	4.91 (0.006)
BP86	2.80	3.64 (0.13)	4.08 (0.049)
M06	2.92	3.89 (0.32)	4.98 (0.006)
PBE1PBE	2.80	3.93 (0.27)	4.89 (0.012)
LC-wPBE	2.80	4.11 (0.26)	5.11 (0.003)
CASPT2/CASSCF(2/12)/ANO-RCC	3.00; 2.96	4.01 (0.66); 4.08 (0.63)	6.21 (0.028); 6.22 (0.032)
CASPT2/CASSCF(2/12)/ECP-Dolg	2.87; 2.83	3.93 (0.70); 4.00 (0.67)	5.91 (0.02); 5.93 (0.02)
EOM-CCSD[b]/Experiment		~4.10[b]/~ 4.2[a]	

[a] Ref. [5]; [b] Ref. [15].

3.3. Ag_4 Tretramer

There are two stable structures for the neutral silver tetramer Ag_4 which are rhombic D_{2h} and Y- shaped C_{2v} structures. Calculated results listed in Table 4 show that the rhombic D_{2h} is more stable than the Y-shaped structure. This result agrees well with previous calculations [15]. TD-DFT and CASPT2/CASSCF calculations have also been used to simulate the absorption spectra of the Ag_4 neutral cluster in both shapes. The energies as well as the oscillator strengths of the vertical electronic transitions for the two structures of Ag_4 are listed in Table 4 and Table 5.

The absorption spectrum of the rhombic Ag_4 (D_{2h}, ^1A_g) in the UV-VIS region is characterized by several bands. The most intense band is centered at ~2.9-3.0 eV, as predicted by both TD-DFT and CASPT2/CASSCF(4/16) calculations. These are close to the experimental result of 3.07 eV [6] and previous calculated results of 3.0 eV [15]. This band is well described by all functionals used and is due to the dominant transition $S_0 \rightarrow S_3$. The other less intense band is found to be centered at ~4.0 eV. The experimental spectrum of Ag_4 shows three well-defined and narrow bands located at 3.07, 4.05 and 4.50 eV [6]. These bands can well be described by our TD-DFT, as well as the CASPT2 calculations, as it could be seen from Table 5. Experimental results [6] led to the assignment that for Ag_4, the rhombic structure D_{2h} is the only

isomer in the Ar noble gas matrix, even though the Y-shaped isomer lies at only ~0.2 eV above the rhombic structure, according to our DFT calculations (Table 5).

3.4. Ag_6 Cluster

Three stable isomers have been found by our calculations, which are in D_{3h}, C_{5v} and C_{2v} point groups. Table 4 shows that DFT calculations using six functionals are consistent, and the planar D_{3h} structure is the most stable isomer of the neutral silver hexamer Ag_6. This finding is in line with previous calculated results [6,7].

Table 4. Relative energies (RE, eV) between the isomers of Ag_4, Ag_6 and Ag_8 neutral clusters calculated using different DFT functionals and the aug-cc-pVDZ-PP basis set.

Functional	Ag_4-Neutral, RE		Ag_6-Neutral, RE			Ag_8-Neutral, RE	
	 , D_{2h}	 , C_{2v}	 , D_{3h}	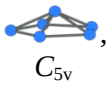 , C_{5v}	 , C_{2v}	 , T_d	 ,D_{2d}
B3LYP	0.00	0.12	0.00	0.31	0.31	0.00	0.085
CAM-B3LYP	0.00	0.19	0.00	0.36	0.37	0.00	0.18
BP86	0.00	0.19	0.00	0.27	0.29	0.00	0.03
M06	0.00	0.24	0.00	0.16	0.29	0.00	-0.04
PBE1PBE	0.00	0.22	0.00	0.23	0.30	0.00	0.09
LCWPBE	0.00	0.30	0.00	0.37	0.41	0.00	0.32

Table 5. Energies (eV) of the vertical electronic transition from the ground state (GS) to the lowest-lying singlet excited states for both rhombic D_{2h} and Y shaped C_{2v} structures of Ag_4. The oscillator strengths (*f*) are given in parentheses. Results are obtained from TD-DFT and CASPT2/CASSCF(4/16) calculations.

	Ag_4, D_{2h} structure			Ag_4-C_{2v} structure	
Method	S_1 (*f*)	S_2 (*f*)	S_3 (*f*)	S_1 (*f*)	S_2(*f*)
B3LYP	1.02 (0.0)	2.76 (0.0)	2.95 (0.81)	1.11 (0.003)	2.69 (0.68)
CAM-B3LYP	1.18 (0.0)	2.72 (0.0)	2.99 (0.86)	1.53 (0.004)	2.79 (0.75)
BP86	1.04 (0.0)	2.90 (0.0)	2.91 (0.57)	0.95 (0.002)	2.54 (0.21)
M06	1.05 (0.0)	2.68 (0.0)	2.89 (0.85)	1.21 (0.006)	2.69 (0.76)
PBE1PBE	1.12 (0.0)	2.72 (0.0)	2.99 (0.87)	1.24 (0.003)	2.72 (0.71)
LC-wPBE	1.44 (0.0)	2.68 (0.0)	3.02 (0.85)	1.99 (0.002)	2.89 (0.77)
CASPT2 (ECP-Dolg)	1.28 (0.0)	2.50 (0.0)	2.89 (1.29)	1.34 (0.005)	2.46 (1.01)
Previous calculations			3.07[a]; 3.21(1.1)[b]; 3.01[c];3.03[d]		2.9 (1.06)[e]

[a] Experimental value, Ref. [12]; [b] Ref. [15]; [c] Ref. [16]; [d] Ref. [17].

TD-DFT has also been used to simulate the absorption spectra of the neutral cluster Ag_6 in all three structures and the calculated results are represented in Table 6 and Figure 2. The experimental spectrum of Ag_6 recorded in argon matrix shows two distinct double peaks centered at 3.63 and 4.15 eV [6]. Harb et al. [6] reported that their calculated results using the

TD-BP86/LANL2DZ level for the lowest-energy planar isomer D_{3h} were not in good agreement with the experimental spectrum. The 3D C_{5v} structure has been proposed to be present in the experimental measurement since it has the main absorption band at 3.65 eV (TD-BP86/LANL2DZ) [6], even though it lies at 0.24 eV higher in energy than the D_{3h} structure. Our TD-DFT calculations using the TD-BP86/aug-cc-pVDZ-PP method show similar results, as it could be seen from the excited state S_4 energy in Table 6. The absorption spectrum of the planar C_{2v} structure, which lies at ~0.3 eV higher energy than the most stable D_{3h} structure (Table 4), is calculated at the B3LYP/aug-cc-pVDZ-PP level and plotted in Figure 2b, in combination with the absorption spectra of the D_{3h} and C_{5v} isomers. Surprisingly, absorption of the C_{2v} structure (red curve in Figure 2b), shows not only a strong band centered at ~3.3 eV but also a less intense band at ~4.4 eV. These results lend a support for the viewpoint that both planar D_{3h} and 3D C_{5v} structures are likely to exist during the experimental absorption measurement of Ag_6, since the latter shows an intense absorption peak at 3.63 eV in the Argon matrix [6, 7]. Moreover, the higher energy planar C_{2v} structure should not be excluded. The blue shift of the experimental absorption could again be due to the effects of the noble gas matrix. A convolution of the calculated absorption spectra of all D_{3h}, C_{5v} and C_{2v} structures of the free-standing Ag_6 neutral cluster shall not reproduce the other intense absorption band located at around 4.15 eV of this neutral hexamer in Argon matrix [6]. Furthermore, as far as we are aware, in the Neon matrix experiment [7], the absorption band at 4.15 eV is not visible, and the most intense absorption band is red-shifted as compared to that in Argon matrix, being centered at 3.45 eV in Ne. We would come to a conclusion that the optical absorption of Ag_6 is rather sensitive to the experimental environments.

3.5. Ag_8 cluster

For the octamer Ag_8, two stable isomers have been found by our calculations and both have 3D structures. The first isomer is in tetrahedral T_d and the second is in D_{2d} point group. DFT results presented in Table 4 show that the tetrahedral T_d structure is the most stable isomer of the neutral silver octamer Ag_8, even though the D_{2d} structure lies only ~0.1 eV higher energy. This finding is in line with the previous calculated results [6, 7].

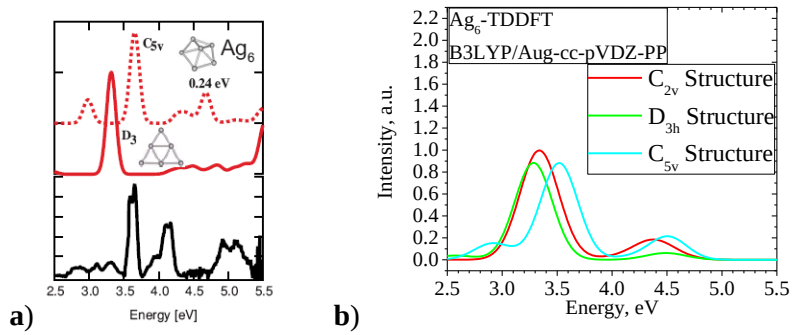

Figure 2. a) Experimental absorption spectrum of the neutral Ag_6 cluster in Ar matrix (the black curve) and the previuos TD-DFT calculated spectrum using BP86/LANL2DZ (the red curve) [6]; b) TDB3LYP/aug-cc-pVDZ-PP calculated absorption spectrum of three Ag_6 isomers in D_{3h}, C_{2v} and C_{5v} symmetry.

The absorption spectrum of neutral silver octamer Ag_8 in T_d have been investigated in detailed [35]. In this research, we would like to briefly discuss the absorption of both T_d and D_{2d} structures. For the purpose of comparison, the experimental and previously calculated spectra are

displayed in Figure 3a. The absorption of the T_d Ag_8 induces the appearance of two bands, a strong band centered at ~3.9 eV and a less intense band located at ~3.0 eV, as shown by the green curve in Figure 3b. The absorption of the D_{2d} structure gives rise to three peaks, the strongest one is also centered at ~3.9 eV, while the less intense bands are located at ~3.1 and ~3.5 eV, respectively. Overall, a convolution of the calculated absorption of both isomers of Ag_8 reproduces quite well the experimental electronic spectra of Ag_8 in both Ar and Ne matrices [6,7]. The lower sensitivity to the matrix environment is due to the high stability of the octamer that a complete electronic shell mimicking the noble gas atoms [35].

Table 6. Energies (eV) of vertical electronic transitions from the ground state to some singlet excited states for both D_{3h} and C_{5v} structures of Ag_6. Experimental results and previous calculations are also listed.

Method	**Ag_6, D_{3h} structure**				**Ag_6-C_{5v} structure**			
	S_1	S_2 (*f*)	S_3	S_4 (*f*)	S_1	S_2 (*f*)	S_3 (*f*)	S_4 (*f*)
B3LYP	2.70	2.57(0.0)	2.86	3.29(0.9)	2.07	2.40	2.92(0.15)	3.52(0.88)
CAM-B3LYP	2.88	2.89(0.1)	3.23	3.42(0.8)	2.26	2.46	3.00(0.14)	3.54(0.96)
BP86	2.66	2.46(0.0)	2.76	3.16(0.6)	2.00	2.35	2.85(0.16)	3.49(0.53)
M06	2.70	2.60(0.1)	2.80	3.26(1.0)	2.02	2.39	2.90(0.14)	3.48(0.95)
PBE1PBE	2.79	2.68(0.1)	2.96	3.35(0.9)	2.16	2.45	2.94(0.11)	3.53(0.97)
LC-wPBE	2.97	3.14(0.3)	3.61	3.58(0.7)	2.55	2.47	3.11(0.15)	3.55(0.95)
Previous calc./Exp.				3.69[b]; 3.24[c]; 3.39[d]/ 3.63[a,*]				3.63[*,a]

(*) This experimental value has not been assigned yet for isolated isomer D_{3h} or C_{5v}, but rather from a convolution of the absorption bands of many possible structures. [a] Ref. [6]; [b] Ref. [15]; [c] Ref. [16]; [d] Ref. [17].

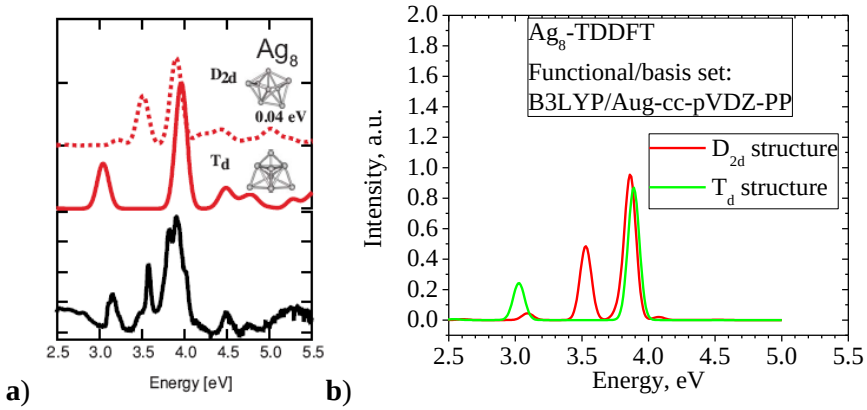

Figure 3. a) Experimental absorption spectrum of neutral Ag_8 cluster in Ar matrix (the black curve) and previous TD-DFT calculated spectrum (the red curve). This figure is taken from Ref. [6]; b) Calculated absorption spectrum of two T_d and D_{2d} isomers of Ag_8 using TD-DFT/B3LYP/aug-cc-pVDZ-PP.

4. CONCLUSION

In the present work, we applied the two main quantum chemical methods, namely the time-dependent density functional theory (TD-DFT) using six representative functionals and the complete active space CASPT2/CASSCF methods, to investigate the electronic structures, some

thermochemical parameters and mostly the absorption spectra of some pure silver clusters Ag_n in the gas phase.

There is an overall fair agreement, where comparison is possible, between TD-DFT and CASPT2 results for transition energies. Where possible, the experimental spectra of the Ag_n clusters examined can reasonably be simulated using the excitation energies obtained either by TD-DFT or CASPT2 method. It is also noteworthy to mention that for some clusters, the neutral Ag_6 for instance, the effects of environment are significant, while for some others such as the neutral Ag_8, they are not.

Acknowledgement. We would like to thank the Ministry of Science and Technology of Vietnam under the project 103.02-2014.67. NTC thanks the Department of Chemistry, University of Leuven, Belgium for he has used its computing facilities.

REFERENCES

1. Díez I. and Ras R. H. A. - Fluorescent silver nanoclusters, Nanoscale **3** (2011) 1963.
2. Sungmoon C., Dickson R. M. and Yu J. - Developing luminescent silver nanodots for biological applications, Chem. Soc. Rev. **41** (2012) 1867.
3. Daniel M.-C. and Astruc D. - Gold nanoparticles: assembly, supramolecular chemistry, quantum-size-related properties, and applications toward biology, catalysis, and nanotechnology, Chem. Rev., **104** (2004) 293.
4. De Cremer G., Antoku Y., Roeffaers M. B. J., Sliwa M., Van Noyen J., Smount S., Hofkens J., De Vos D. E., Sels B. F. and Vosch T - Photoactivation of silver-exchanged zeolite A, Angew. Chem. Int. Ed., **47** (2008) 2813.
5. Lecoultre S, Rydlo A. and Félix C. - Efficient trapping of silver cations in a rare gas matrix: Ag_3^+ in argon, J. Chem. Phys., **126** (2007) 204507.
6. Harb M., Rabilloud F., Simon D., Rydlo A., Lecoultre S., Conus F., Rodrigues V. and Félix C. - Optical absorption of small silver clusters: Ag_n, (n=4-22), J. Chem. Phys., 129 (2008) 194108.
7. Lecoultre S., Rydlo A., Buttet J., Félix C., Gilb S. and Harbich W. - Ultraviolet-visible absorption of small silver clusters in neon: Ag_n (n = 1-9), J. Chem. Phys., **134** (2011) 184504.
8. Handschuh H., Cha C. Y., Bechthold P. S., Gantefor G. and Eberhardt W. - Electronic shells or molecular orbitals: photoelectron spectra of Ag_n^- clusters, J. Chem. Phys., **102** (1995) 6406.
9. Beutel V., Kramer H.-G., Bhale G. L., Kuhn M., Weyers K. and Demtroder W. - High-resolution isotope selective laser spectroscopy of Ag_2 molecules, J. Chem. Phys., **98** (1993) 2699.
10. Jackschath C., Rabin I. and Schulze W. - Electron impact ionization of silver clusters Ag_n, $n \leq 36$, Z. Phys. D, **22** (1992) 517.
11. Ruamps P. J. - Spectre d'emission des molecules Cu_2, Ag_2, et Au_2, Compt. Rend., **238** (1954) 1489.
12. Ruamps P. J. - Production et etude du spectre optique de molecules diatomiques de metaux et contribution au calcul theorique des intensites, Ann. Phys. (Paris), **4** (1959)

1111.

13. Maheshwari R. C. - New band systems of Ag_2 molecule in the far ultra-violet region, Indian J. Phys., **37** (1963) 368.
14. Shin-Piaw C., Loong-Seng W. and Yoke-Seng L. - Emission band systems of Ag_2 produced in discharge, Nature (London), **209** (1966) 1300.
15. Bonačić-Koutecký V., Pittner J., Boiron M. and Fantucci P. - An accurate relativistic effective-core-potential for excited states of Ag-atom; Application to study of the absorption spectra of Ag_n and Ag_n^+ clusters, J. Chem. Phys., **110** (1999) 3876.
16. Idrobo J. C., Ogut S. and Jellinek J. - Size dependence of static polarizabilities and absorption spectra of gold clusters, Phys. Rev. B, **72** (2005) 085445.
17. Zhao G. F., Lei Y. and Zeng Z. - Research optical characteristics of H_2S molecule adsorption on Ag_n (n = 2,4,6) clusters, Chem. Phys., **327** (2006) 261.
18. Janssens E., Hou X. J., Nguyen M. T. and Lievens P. - The geometric, electronic, and magnetic properties of Ag_5X^+ (X = Sc, Ti, V, Cr, Mn, Fe, Co, and Ni) clusters, J. Chem. Phys., **124** (2006) 184319.
19. Bauernschmitt R. and Ahlrichs R. - Treatment of electronic excitations within the adiabatic approximation of time dependent density functional theory, Chem. Phys. Lett., **256** (1996) 454.
20. Casida M. E., Jamorski C., Casida K. C. and Salahub D. R. - Molecular excitation energies to high-lying bound states from time-dependent density functional theory: Characterization and correction of the time-dependent local density approximation ionization threshold, J. Chem. Phys., **108** (1998) 4439.
21. Furche F. and Ahlrichs R. - Adiabatic time-dependent density functional methods for excited state properties, J. Chem. Phys., **117** (2002) 7433.
22. Scalmani G., Frisch M. J., Mennucci B., Tomasi J., Cammi R. and BaroneV. - Geometries and properties of excited states in the gas phase and in solution: Theory and application of a time-dependent density functional theory polarizable continuum model, J. Chem. Phys., 124 (2006) 094107.
23. Marques M. A. L., Maitra N. T., Nogueira F. M. S., Gross E. K. U. and Rubio A. - Fundamentals of time-dependent density functional theory, Springer-Verlag Berlin Heidelberg, 2012.
24. Frisch M. J., Trucks G. W., Schlegel H. B., Scuseria G. E., Robb M. A., Cheeseman J. R.,Scalmani G., Barone V., Mennucci B., Petersson G. A., Nakatsuji H., Caricato M., Li X., Hratchian H. P., Izmaylov A. F., Bloino J., Zheng G., Sonnenberg J. L., Hada M., Ehara M., Toyota K., Fukuda R., Hasegawa J., Ishida M., Nakajima T., Honda Y., Kitao O., Nakai H., Vreven T., Montgomery J. A., Peralta J. E., Ogliaro F., Bearpark M., Heyd J. J., Brothers E., Kudin K. N., Staroverov V. N., Kobayashi R., Normand J., Raghavachari K., Rendell A., Burant J. C., Iyengar S. S., Tomasi J., Cossi M., Rega N., Millam J. M., Klene M., Knox J. E., Cross J. B., Bakken V., Adamo C., Jaramillo J., Gomperts R., Stratmann R. E., Yazyev O., Austin A. J., Cammi R., Pomelli C., Ochterski J. W., Martin R. L., Morokuma K., Zakrzewski V. G., Voth G. A., Salvador P., Dannenberg J. J., Dapprich S., Daniels A. D., Farkas O., Foresman J. B., Ortiz J. V., Cioslowski J., and Fox D. J., GAUSSIAN 09, Revision A.02, Gaussian, Inc. Wallingford, CT, 2009.

25. Karlström G., Lindh R., Malmqvist P.-Å., Roos B. O., Ryde U., Veryazov V., Widmark P.-O., Cossi M., Schimmelpfennig B., Neograd y P. and Seijo L. - MOLCAS: a program package for computational chemistry, Comput. Mater. Sci., **28** (2003) 222.
26. Becke A. D. -Density-functional thermochemistry. III. The role of exact exchange, J. Chem. Phys., **98**(1993) 5648.
27. Yanai T., Tew D. and Handy N. - A new hybrid exchange–correlation functional using the Coulomb-attenuating method, Chem. Phys. Lett., **393** (2004) 51.
28. Perdew J. P. - Density-functional approximation for the correlation energy of the inhomogeneous electron gas, Phys. Rev. B, **33** (1986) 8822.
29. Zhao Y. and Truhlar D. G. - The M06 suite of density functionals for main group thermochemistry, thermochemical kinetics, noncovalent interactions, excited states, and transition elements: two new functionals and systematic testing of four M06-class functionals and 12 other functionals, Theor. Chem. Acc., **120** (2008) 215.
30. K. Burke, M. Ernzerhof and J. P. Perdew - Why semilocal functionals work: Accuracy of the on-top pair density and importance of system averaging, J. Chem. Phys., **109** (1998) 3760.
31. Vydrov O. A. and Scuseria G. E. - Assessment of a long-range corrected hybrid functional, J. Chem. Phys., **125** (2006) 234109.
32. Peterson K.A. and Puzzarini C. - Systematically convergent basis sets for transition metals. II. Pseudopotential-based correlation consistent basis sets for the group 11 (Cu, Ag, Au) and 12 (Zn, Cd, Hg) elements, Theor. Chem. Acc., **114** (2005) 283.
33. Roos B. O., Lindh R. and Malmqvist P.-A., Veryazov V. and Widmark P.-O. - New Relativistic ANO Basis Sets for Transition Metal Atoms, J. Phys. Chem. A, 109 (2005) 6575.
34. Andrae D, Häußermann U., Dolg M., Stoll H. and Preuß H. - Energy-adjusted ab initio pseudopotentials for the second and third row transition elements, Theor. Chem. Acc., **77** (1990) 123.
35. Cuong N. T., Nguyen H. M. T., Nguyen M. T. - Theoretical modeling of optical properties of Ag_8 and Ag_{14} silver clusters embedded in an LTA sodalite cavity, Phys. Chem. Chem. Phys., **15** (2013) 15404.